CECA-D-15-00101. R1

The two pore channel TPC2 is dispensable in pancreatic β-cells for normal Ca^{2+} dynamics and insulin secretion

Matthew C. Cane[a], John Parrington[b], Patrik Rorsman[c], Antony Galione[b] and Guy A. Rutter[a]*

[a]Section of Cell Biology and Functional Genomics, Imperial College London, DuCane Road W12 0NN, London, UK

[b]Department of Pharmacology, University of Oxford, Mansfield Road, OX1 3QT, UK

[c]The Oxford Centre for Diabetes, Endocrinology and Metabolism, Churchill Hospital, Oxford OX3 7LJ, United Kingdom.

*To whom correspondence should be addressed: g.rutter@imperial.ac.uk

Abstract.

Ca^{2+} signals are central to the stimulation of insulin secretion from pancreatic β-cells by glucose and other agents, including glucagon-like peptide-1 (GLP-1). Whilst Ca^{2+} influx through voltage-gated Ca^{2+} channels on the plasma membrane is a key trigger for glucose-stimulated secretion, mobilization of Ca^{2+} from acidic stores has been implicated in the control of more localised Ca^{2+} changes and membrane potential. Nicotinic acid adenine dinucleotide phosphate (NAADP), generated in β-cells in response to high glucose, is a potent mobilizer of these stores, and has been proposed to act through two pore channels (TPC1 and TPC2, murine gene names *Tpcn1* and *Tpcn2*). Whilst the role of TPC1 in the control of Ca^{2+} mobilization and insulin secretion was recently confirmed, conflicting data exist for TPC2. Here, we used the selective and efficient deleter strain, Ins1*Cre* to achieve β-cell selective deletion of the *Tpcn2* gene in mice. βTpcn2 KO mice displayed normal intraperitoneal and oral glucose tolerance, and glucose-stimulated Ca^{2+} dynamics and insulin secretion from islets were similarly normal. GLP-1-induced Ca^{2+} increases involved an increase in oscillation frequency from 4.35 to 4.84 per minute (p=0.04) at 8 mM glucose, and this increase was unaffected by the absence of *Tpcn2*. The current data thus indicate that TPC2 is not absolutely required for normal glucose- or incretin-stimulated insulin secretion from the β-cell. Our findings suggest that TPC1, whose expression tended to increase in *Tpcn2* null islets, might be sufficient to support normal Ca^{2+} dynamics in response to stimulation by nutrients or incretins.

Keywords: β-cell, calcium, TPC2, diabetes, GLP-1, NAADP

Abbreviations: AUC, area under the curve; $[Ca^{2+}]_i$, intracellular free Ca^{2+} ion concentration; GLP-1, glucagon-like peptide-1; IPGTT, OGTT, intraperitoneal and oral glucose tolerance test; NAADP, nicotinic acid adenine dinucleotide phosphate; TPC1, TPC2, two pore channels 1 and 2

Introduction

The pancreatic islet β-cell is an important model for the study of fuel sensing and stimulus-secretion coupling [1, 2]. Derangement of normal β-cell function [3], as well as a decrease in overall β-cell mass [4, 5], underlie insulin deficiency in type 2 diabetes [1, 6, 7] a disease which now affects more than 8 % of the adult population worldwide [8].

Classically, elevated blood glucose levels are believed to stimulate insulin secretion through an increased cytosolic ATP:ADP ratio [9, 10] leading to closure of ATP-sensitive K^+ channels (K_{ATP}) [11] and enhanced Ca^{2+} influx through voltage-dependent Ca^{2+} channels (VDCCs). Whilst substantial pharmacological [11] and genetic [12, 13] evidence supports this model, it is undoubtedly incomplete, not least because deletion of K_{ATP} channel subunits (SUR1/*ABCC8* and Kir6.2/*KCNJ11*) does not render β-cells wholly glucose-unresponsive [14, 15]. Indeed, it is increasingly accepted that an integration of nutrient, neurotransmitter and hormonal signals is necessary for the induction of insulin release *in vivo* [1, 2].

Internal Ca^{2+} stores, including those associated with the endoplasmic reticulum (ER) [16], and acidic stores, are also known to modulate intracellular free Ca^{2+} ($[Ca^{2+}]_i$) signals in β-cells [2]. Of note, alkalinisation of acidic stores by inhibition of the V_o-ATPase with Bafilomycin A1 impedes glucose-induced $[Ca^{2+}]_i$ responses in these cells [17, 18]. Nicotinic acid adenine dinucleotide (NAADP) is an important second messenger which has been implicated in the recruitment of acidic stores for the generation of $[Ca^{2+}]_i$ signals. Produced by the endosomal/cell surface-located enzyme CD38 via a base exchange reaction [19], NAADP is generated in β-cells in response to glucose [20], and the incretin hormone glucagon-like peptide-1 (GLP-1) [21]. Whilst the latter G-protein receptor-coupled hormone potently stimulates insulin secretion at permissive glucose concentrations, allowing the development of incretin-based therapies for type 2 diabetes [22-24], the impact of GLP-1 on β-cell Ca^{2+} dynamics is less well established and appears to be species dependent [25-27].

Whilst also a matter of debate, consensus is building that one or more of the two pore channel subtypes (TPC) serves as the putative NAADP receptor Ca^{2+}-release channel. Nevertheless, it is also possible that TPCs form one part of a channel complex that also includes a distinct NAADP-binding protein. Expressed on endo-lysosomal compartments, TPCs (gene name *TPCN*) have been implicated in the generation of NAADP-mediated Ca^{2+} signals in β- and other cells. Thus, TPC2 expression renders NAADP-unresponsive cells responsive [28], and expression of cell surface targeted TPCs allows NAADP to induce Ca^{2+} influx [29]. Furthermore, both the rodent *Tpcn2* and the orthologous human *TPCN2* gene have been identified as potential causal genes for diabetes-associated traits [30].

Despite this body of data indicating an important role of TPC2 in Ca^{2+} signalling in β-cells, knock out of the *Tpcn2* gene in various animal models has shown divergent effects. For example, global deletion of the *Tpcn2* gene in the mouse through the use of a gene trap vector renders pancreatic β-cells unresponsive to NAADP either through use of the cell permeable analogue NAADP-AM or through introduction of NAADP directly through the patch pipette [17, 28]. Similarly, glucose-induced Ca^{2+} signals are also somewhat impaired in *Tpcn2*$^{-/-}$ mice, although they are not fully ablated [17]. Nonetheless, glucose-induced insulin secretion was barely affected and glucose tolerance was not abnormal in *Tpcn2*$^{-/-}$ animals [17]. On the other hand, *Tpcn1*$^{-/-}$ mice showed clear differences in both parameters [17]. Of note, although the *Tpcn2*$^{-/-}$ mice used in a recent study by Wang et al. [18]

similarly failed to show any abnormalities in terms of responses to NAADP, the truncation in this allele may still enable the expression of a functional TPC2 protein [31].

In light of these discrepancies, we have generated β-cell-specific *Tpcn2* knockout mice by crossing animals harbouring a *flox*ed exon of the *Tpcn2* gene to knock-in mice expressing *Cre* recombinase at the endogenous *Ins1* locus [32, 33]. This strategy results in efficient (~95%) recombination in β-cells [32, 33] (Johnston et al, unpublished results) throughout the islet. Furthermore, and in contrast to other currently-available insulin promoter-driven *Cres*, notably RIP2Cre [34-36], recombination with the Ins1*Cre* strain is not complicated either by off-target events including recombination in the brain [37] nor by the simultaneous ectopic expression of human growth hormone (hGH) in the β-cell.

This approach has enabled us to further study the role of TPC2 in the β-cell whilst eliminating confounding effects which may result from the deletion of the *Tpcn2* gene in other tissues. After confirming ablation of *Tpcn2* expression we have used this model to determine the cell autonomous role of TPC2 in the β-cell, focussing on glucose homeostasis, insulin secretion and the regulation of Ca^{2+} dynamics by glucose and incretins.

2. Methods

2.1 Animal origin and maintenance

Mice heterozygous for the *flox*ed allele of the *Tpcn2* gene (exon 6 flanked by *lox*P sites) were obtained from the European conditional mouse mutagenesis program (EUCOMM) via MRC Harwell, U.K. Mice bore the "Tm1c" (http://www.mousephenotype.org/about-ikmc/eucomm-program/eucomm-targeting-strategies) allele ($Tpcn2^{tm1c(EUCOMM)Hmgu}$) and were crossed with Ins1Cre-expressing animals [32]. The subsequent litters were back-crossed to generate $Tpcn2^{fl/fl}$:$Ins1Cre^{+/-}$ (referred to as 'KO') and $Tpcn2^{fl/fl}$:$Ins1Cre^{-/-}$ (referred to as 'control') mice. Offspring were bred together to generate litters with ~50 % WT mice and ~50% β-cell specific *Tpcn2*-deleted mice. Animals bearing the Ins1Cre transgene alone displayed no abnormalities in glucose tolerance, insulin secretion or β-cell mass [32].

Animals were maintained on a C57/BL6 background and 2 to 4 mice were housed per individually-ventilated cage in a pathogen-free facility. Mice were kept under a 12 h light/dark cycle and fed a regular chow diet (Lillico Biotechnology). All *in vivo* experiments were performed on male mice and islets were isolated from an equal number of male and female mice. All animal experiments were approved by the UK Home Office under the Animals (Scientific Procedures) Act 1986 (PPL 70/7349).

2.2 qRT-PCR

Approximately 100 freshly isolated islets were used for RNA extraction using TRIzol reagent (Invitrogen) and cDNA was generated using a high capacity reverse transcription kit (Applied Biosystems) according to the manufacturer's instructions. SYBR Green qRT-PCR was performed as previously described (REF) and β-Actin was used as the reference gene.

2.3 Glucose Tolerance Tests

Mice were fasted overnight before i.p. injection or oral gavage of 30% glucose in water to a dose of either 1g/kg or 3g/kg. Blood was sampled from the tail vein at 0, 15, 30, 60 and 120 min and glycaemia measured using an automatic glucometer (Accu-chek, Roche).

2.4 Insulin Secretion

Islets were isolated by collagenase dissociation as described previously [38] and ~50 islets were perifused with Krebs-HEPES buffer (in mM, 130 NaCl, 3.6 KCl, 0.5 NaH_2PO_4, 2 $NaHCO_3$, 1.5 $CaCl_2$, 1.2 $MgCl_2$, 3 D-glucose, 10 HEPES, 0.5 $MgSO_4$, pH 7.4 substituted with 0.1% bovine serum albumin) at a rate of 500 µl min^{-1} at 37 °C in a custom-built chamber. Perifusate was collected in 30 s intervals. Islets were primed with Krebs medium containing 3 mM glucose for 30 minutes prior to the experiment and glucose was increased to 16.9 mM 2 min. after the initial collection. Islets were then frozen in 10 ml acidic ethanol (1.5% 1M HCl, 75% EtOH, 0.1% Triton X-100) until assayed for total insulin content. The latter samples were diluted 1:100 whilst secreted insulin samples were assayed undiluted using an HTRF insulin assay kit (Cisbio assays) and a PHERAstar reader (BMG), following the manufacturer's guidelines.

2.5 Calcium imaging

Experiments were performed essentially as previously described [26]. In brief, islets were loaded with 10 µM Fluo-8 AM (Abcam) dissolved in DMSO (0.01 % wt/vol) in Krebs-HEPES buffer for 45

minutes at 37 °C. Islets were visualised using a Zeiss Axiovert confocal microscope and perifused continuously at 34-36 °C with Krebs-HEPES buffer containing relevant concentrations of glucose and GLP-1. Fluo-8 was excited with a 491 nm laser and emitted light collected at 525 nm. Volocity™ software (Perkin-Elmer) was used for imaging and analysis. Traces were normalised to the initial fluorescence (F/F_0).

2.6 Statistics

Data were analysed using GraphPad PRISM 6.0 software and significance was tested using unpaired Student's two-tailed t-tests with Bonferroni post-tests for multiple comparisons, or two-way ANOVA as indicated. $P<0.05$ was considered significant and errors signify mean ± SEM.

3. Results

3.1 Unaltered glucose tolerance after targeted deletion of Tpcn2 from β-cells.

To delete TPC2 specifically from the pancreatic β-cell, mice bearing alleles of the *Tpcn2* gene with *lox*P sites flanking exon 6 were crossed to mice bearing the Ins1*Cre* transgene [32]. In the first instance, we confirmed the *Cre* excision event by PCR. Primers flanking the *lox*P sites were expected to generate a 1055 bp fragment in the control islets, and a smaller fragment of 215 bps in the KO islets, after the excision event has taken place. The corresponding bands can be seen in Figure 1B. Secondly, we confirmed knock down of the expression of *Tpcn2* by qRT-PCR. Relative expression of the Tpcn2 transcript from KO islets was decreased to ~50% of control levels. This reduction is compatible with essentially complete deletion from β-cells, assuming a β- : α-cell ratio of ~3:1 [39] and a ratio of *Tpcn2* mRNA of 1:3 in β- : α-cells [40]. *Tpcn1* mRNA levels showed a slight tendency towards an increase in *Tpcn2* null islets (p= 0.147, Fig. 1C)

β*Tpcn2* KO mice were indistinguishable from littermate control animals by visual inspection, and displayed normal growth and weight changes (Fig. 1D). Glucose tolerance was investigated in these mice by both intraperitoneal (IPGTT) and oral (OGTT) administration of the sugar, the latter allowing exploration of the incretin effect on insulin secretion. Mice underwent IPGTTs at 8-12 weeks, and then again at 16-20 weeks of age by administration of 1 g/kg glucose. Whilst a small decrease in glucose tolerance was observed between the younger and older mice, no significant differences were observed between the β*Tpcn2* KO mice and their littermate controls in either age group (Fig. 2A, B). Similarly, no significant difference between genotypes was observed during either OGTT at 12-16 weeks (performed using a higher concentration of 3 g/kg glucose) or at 20-24 weeks of age (Fig. 2B, C).

3.2 Normal glucose-induced Ca^{2+} dynamics and insulin secretion in βTpcn2 KO mouse islets

Having demonstrated a lack of any effect of β-cell selective TPC2 ablation on glucose tolerance *in vivo*, where compensatory effects might conceivably obscure changes in β-cell glucose responsiveness, we performed studies using islets *ex vivo* to determine whether a more subtle role of TPC2 deletion might be unmasked. The effect of TPC2 deletion in β-cells on Ca^{2+} signals was investigated by live fluorescence microscopy on isolated islets loaded with the Ca^{2+} indicator Fluo-8. Peak-plateau responses in intracellular free Ca^{2+} ($[Ca^{2+}]_i$) were generated in whole islets by the addition of high (17 mM) glucose after a period of exposure to low (3 mM) glucose. Regions of interest were drawn around the whole islet to observe the coordinated response to increased glucose. TPC2 deletion had no obvious effect on the above Ca^{2+} responses, after analysis of both the peak and the area under curve (AUC). Likewise, changes in membrane potential after high glucose treatment were similarly not affected by the absence of TPC2 (Sones, W and RP, results not shown, *n*=3).

Insulin secretion from isolated islets was next monitored dynamically over time using a custom built perifusion apparatus. Insulin secretion was induced by the addition of 17 mM glucose after a period of exposure to low glucose (3 mM). Insulin secretion began immediately after the increase in glucose concentration and achieved a peak rate of secretion of approximately 0.14% of the total insulin content per minute. Secretion then slowed to a plateau around 0.07% of total insulin per minute. The absence of TPC2 from β-cells resulted in no evident change in either the peak rate of this response nor in the overall insulin secreted, as represented by analysis of the area under the curve.

3.3 Normal incretin-induced Ca^{2+} dynamics and insulin secretion in βTpcn2 KO mouse islets

We next used the same techniques to determine whether TPC2 may contribute to incretin-regulated Ca^{2+} dynamics. Islets were stimulated first with 11 mM glucose and additionally with 20 nM GLP-1 eight minutes later. Addition of the incretin at this concentration of glucose did not lead to any significant effect on $[Ca^{2+}]_i$ in control or KO islets. However, and despite not significantly affecting Ca^{2+} signals, GLP-1 did induce a rapid and significant increase in the plateau of insulin secretion, indicating that the ability of GLP-1 to increase insulin release was via potentiation of Ca^{2+}-dependent exocytosis but did not result from an increase in $[Ca^{2+}]_i$ beyond that produced by glucose alone. TPC2 ablation did not affect the secretory response to GLP-1, nor insulin secretion in response to 8 mM glucose alone, as confirmed by area under the curve analysis and measurement of peak responses.

3.4 Subtle changes in GLP-1-induced Ca^{2+} transients during moderate glucose stimulation of βTpcn2 KO islets are indistinguishable from control

In an attempt to investigate a more subtle role of GLP-1 in Ca^{2+} signalling and to subsequently investigate the role of TPC2 in this response, we induced stable Ca^{2+} oscillations in isolated mouse islets by stimulating with 8 mM glucose. The resulting oscillations were variable between islets as can be seen in the individual example traces (Fig. 5 A, B). The oscillations were also systemic across the islet and not specific to individual cells or regions (Fig. 5 C). The addition of GLP-1 after glucose administration increased the frequency of these oscillations without prompting any recruitment of previously quiescent cells into activity (Fig. 5 A–C). Islets showed varying responses to GLP-1 but a significant number showed an increase, as can be seen by the increase in frequency shown in (Fig. 5 D-F). However, no effect of *Tpcn2* deletion on this modulation of Ca^{2+} oscillation frequency was observed.

4. DISCUSSION

4.1 Role of TPC2 in the beta cell

We describe here the impact on glucose homeostasis and Ca^{2+} dynamics of β-cell selective deletion of *Tpcn2* in the mouse. Elimination of TPC2 was confirmed by demonstrating a reduction in transcript level compatible with a selective loss from the β-cell compartment, as expected with the use of the efficient and β-cell-selective Ins1*Cre* strain [32]. Confirmation of knockdown at the protein level was not possible since commercially available antibodies proved to be non-specific in our hands (results not shown).

The use of pharmacological agents (e.g. Bafilomycin A1) to alkalinise this compartment, or others (GPN) to osmotically destabilise it, have provided evidence for the importance of the acidic compartment as a Ca^{2+} store involved in β-cell stimulus secretion coupling [41] as well as in other cell types including neuronal [42] and smooth muscle [43] cells. The specific role for NAADP in accessing these stores has also been shown pharmacologically using competitive inhibition of NAADP-sensing with the putative NAADP-receptor antagonist Ned-19 [17, 20]. The potential role of the two-pore channel as either a direct or indirect component of the NAADP-receptive machinery has also been demonstrated by several groups [44][45][46][47] including ourselves [17, 31].

However, it should be noted that technical differences between studies mean that the current literature from other cells types cannot necessarily be extrapolated directly to the β-cell. Most importantly, pharmacological inhibition may lead to off-target effects. This is especially the case when the function or integrity of an entire organelle is disrupted, as in the case of Bafilomycin A1 or GPN, manoeuvres which have been shown to also block IP_3- and cADPR-mediated signals in Jurkat T-lymphocytes [48]. Likewise, whole-body deletion of a gene which is expressed in other metabolically relevant tissues could have significant subsequent effects on islet function; the *Tpcn* (and particularly *Tpcn2*) family are particularly strongly expressed in hematopoetic lineages in mice (bioGPS.org) and their deletion from these tissues might conceivably affect innate immunity or alter inflammatory status, with subsequent impacts on islet and β-cell function [49].

We therefore chose in the present study to use (1) targeted gene inactivation achieved through *Lox*P-mediated recombination of floxed *Tpcn2* alleles, and (2) investigations of β-cell Ca^{2+} responses in whole islets. The latter preparation provides a reliable means of studying robust and reproducible $[Ca^{2+}]_i$ signals in the absence of changes in β-cell physiology and responsiveness which can accompany islet disruption [26, 27]. Although the Ca^{2+} indicator used, Fluo-8, is not partitioned selectively into β-cells, increases in $[Ca^{2+}]_i$ in response to glucose (or GLP-1) are likely to be restricted to these cells, and a small number of δ-cells, rather than α-cells which comprise ~20% of the islet [26].

Examined in this setting, loss of *Tpcn2* exerted no apparent effect on Ca^{2+} signals provoked by nutrients or incretin. Whilst this may seem to question previous findings on *Tpcn2*$^{-/-}$ mice, it should be emphasised that our earlier studies involved the use of isolated β-cells [17]. It is therefore possible that the involvement of NAADP in glucose responses may be less susceptible to deletion of *Tpcn2* in the context of the intact islet, given the complex communication and feedback mechanisms existing between β-cells within the micro-organ [50].

In contrast, and despite minimal effects of *Tpcn2* deletion on glucose tolerance, glucose-evoked Ca^{2+} responses and insulin secretion [17], responses to infused NAADP were eliminated in β-cells from whole body *Tpcn2*$^{-/-}$ mice. The present data therefore suggest that such currents, activated by high

NAADP, are not required for normal Ca^{2+} oscillations in response to glucose or GLP-1 (see Fig.s 3-5). However, we would note that the present studies did not explore the impact of NAADP in β*Tpcn2* KO mouse islets and it is conceivable that these NAADP-regulated currents persisted, perhaps as a result of up-regulation of *Tpcn1* (Fig. 1C). Alternatively, smaller currents, which cannot be readily detected by patch clamp electrophysiology, may be critical and contribute to local changes in membrane potential which regulate Ca^{2+} influx.

It is conceivable that the tendency for increases in *Tpcn1* expression after *Tpcn2* deletion, as seen in Fig. 1 is sufficient to compensate for the absence of the latter, especially given that basal levels of *Tpcn1* mRNA in the islet are significantly (>10-fold) higher than those of Tpcn2 [17], as also observed in other tissues such as liver [31]. Correspondingly, *Tpcn1*$^{-/-}$ mice show marked defects in both glucose tolerance and in glucose-stimulated insulin secretion. Thus, it is possible that significant functional redundancy exists between TPC1 and TPC2 in the β-cell. Studies using mice deleted for *Tpcn1* alone or both alleles in these cells will be necessary to test this hypothesis.

4.2 GLP-1 and Ca^{2+} dynamics

In the physiologically relevant setting of the perifused whole islet, we observed only rather subtle effects of GLP-1 on Ca^{2+} signals induced by low, stimulatory (8 mM) concentrations of glucose (Fig. 5). These observations are thus compatible with earlier studies [25-27] demonstrating a role for GLP-1 in controlling Ca^{2+} dynamics in β-cells. More noticeable was the complete lack of any observable effect of GLP-1 on Ca^{2+} dynamics induced by both intermediate (11 mM) and elevated (17 mM) glucose concentrations, despite marked increases in insulin secretion under the same conditions (Figs 4, 5). This finding suggests that at these high glucose concentrations GLP-1 principally acts by potentiation of glucose-induced insulin secretion and does not involve an increase in electrical activity or $[Ca^{2+}]_i$. However, at lower glucose concentrations (8 mM), GLP-1 elicited an increase in $[Ca^{2+}]_i$ that likely reflects stimulation of electrical activity. Thus, the mode of action of GLP-1 differs depending on the glucose concentration. Importantly, elimination of *Tpcn2* had no effect on GLP-1-induced changes in Ca^{2+} dynamics or insulin secretion at any of the glucose concentrations tested, arguing against an absolute requirement for these channels in NAADP-mediated effects.

4.3 Overall conclusions

The present studies demonstrate that TPC2 is not absolutely required for normal glucose or incretin responses in pancreatic β-cells. The present studies also suggest that the actions of GLP-1 on insulin secretion occur predominantly, though not exclusively, via mechanisms which are independent of changes in $[Ca^{2+}]_i$. We suggest that there may be significant overlap, and therefore redundancy, between two pore channel subtypes (*Tpcn1* and *Tpcn2*), allowing NAADP-dependent actions to persist. The importance of the NAADP-mediated Ca^{2+}-release pathway may also have been somewhat exaggerated in previous investigations. The use here of a more sophisticated, β-cell-specific deletion model and *in vivo* analyses overcome many of these limitations.

Acknowledgements.

Supported by Wellcome Trust Senior Investigator Awards (WT098424AIA to G.A.R. WT095531/Z/11/Z to P.R. and 102828/Z/13/Z to A.G.), and an MRC Programme Grant (G0901521). G.A.R. is the recipient of a Royal Society Wolfson Research Merit Award.

Table 1. List of primers.

qRT-PCR primers were designed to span an exon boundary in order to prevent interaction with genomic DNA as opposed to cDNA. *Tpcn2* flox primers flank a *lox*P site, producing differential product sizes for *flox*ed and wild type alleles. Excision event primers flank both *lox*P sites allowing for confirmation of the *Cre* excision event.

qRT-PCR	*Tpcn2*	F - ATGATGAAGAAGACCCTGAAGTG R - TGTGCTTCATCCTTCTCACC
	β-actin	F - CGAGTCGCGTCCACCC R - CATCCATGGCGAACTGGTG
Genotyping	*Tpcn2* flox	F - ATTCTGGGCTGCTACTGTGG R - GTTGGTCCTCCTAGGCTGTG
	Ins1cre	F - ATGTCCAATTTACTGACCG R - CGCCGCATAACCAGTGAAAC
Excision event		*F* - CTGCTACTGTGGGTGGTATATGG *R* - CAATGTTATTTGAACTGATGGCGAG

Figure Legends

Figure 1

(A) Schematic of the *flox*ed allele of *Tpcn2* showing the location of *loxP* sites flanking exon 6 and the target sites of primers used in (C). (B) The excision event resulting from the cross with Ins1Cre mice as demonstrated by the removal of the critical region containing exon 6. (C) Relative expression of *Tpcn2* in control (black) and β-cell-specific *Tpcn2* KO (blue) islets, normalised to β-actin (*Actb*). *P<0.05 for the effect of *Tpcn2* deletion. (D) Changes in the weight of control (black) and KO (blue) animals from 8 to 20 weeks of age.

Figure 2

Glucose tolerance tests of control and β*Tpcn2* KO mice. Glucose tolerance after intraperitoneal (ip) glucose injection (A,B) or oral glucose via gavage (C,D) of male mice. Mice were given 1g kg^{-1} glucose with the exception of the 12-16-week OGTT mice (C) which were given a higher dose of 3g kg^{-1}. Experiments were quantified by area under the curve (AUC) analysis as shown in the inset bar graphs and the number of mice used in each experiment is shown in white. Data are expressed as means ± SEM. No statistically significant differences were observed.

Figure 3

Glucose responsiveness of control and β*Tpcn2* KO islets. (A - G) Ca^{2+} responses to 17 mM glucose in control islets (blue) and β-cell specific *Tpcn2* KO islets (black). Example Ca^{2+} responses (A, B), and corresponding images of basal and peak fluorescence showing the global response over the whole islet (C, D) where scale bars correspond to 20 µm. (E) Averaged response showing the mean ± SEM of Ca^{2+} traces. These data are quantified by area under curve analysis (F) and the average peak fluorescence (G). (H-J) Insulin secretion from isolated islets from control (black) and beta cell specific *Tpcn2* knock-out mice (blue). (H) Insulin secreted over time shown as mean ± SEM. Quantification of the insulin secretion during the period from 2-32 minutes after the start of the experiment by total insulin secreted as a percentage of the total insulin content of the islets (I) and peak insulin response (J). The number of islets used for each set of experiments is shown on the bars in white.

Figure 4

Effect of GLP-1 on control and β*Tpcn2* KO islets (A) Average Ca^{2+} responses showing mean ± SEM. (B, C) Quantification of the area under the curve (AUC) and peak of Ca^{2+} traces. (D) Insulin secretion from isolated islets from control (black) and β*Tpcn2* KO mice (blue). (E, F) Quantification of insulin secretion during the period from 2-32 minutes after the start of the experiment for the 17 mM glucose-stimulated islets, or from 10-32 minutes for the 11 mM glucose plus GLP-1-stimulated islets. The number of islets used for each set of experiments is shown on the bars in white.

Figure 5

Effect of GLP-1 on Ca^{2+} oscillations in control and β*Tpcn2* KO islets. (A, B) Example traces of control islets (blue) and β-cell-specific *Tpcn2* KO islets (black), showing Ca^{2+} responses to 8 mM glucose with the addition of GLP-1. Boxes in (B) indicate regions shown in (C). (C) Example Ca^{2+} oscillations before and after the addition of GLP-1 after the 8 mM glucose response in a KO islet. The Ca^{2+} signal, as observed during a single oscillation (image capture at 2 s intervals) is apparent across the whole islet. The increase in oscillation frequency is apparent between the upper (-GLP-1) and

lower (+GLP-1) traces. Scale bar = 20 µm. (D, E) Change in oscillation frequency upon GLP-1 stimulation normalised to the rate induced by 8 mM glucose. Oscillations were counted in a five minute window before and after GLP-1 addition and the red dotted line indicated the average increase. $P<0.05$ for the effects of GLP-1 in each case. (F) Quantification of the increase in oscillation frequency, showing no significant difference between control and β*Tpcn2* KO islets (mean ± SEM).

References

[1] G.A. Rutter, T.J. Pullen, D.J. Hodson, A. Martinez-Sanchez, Pancreatic beta-cell identity, glucose sensing and the control of insulin secretion, Biochem J, 466 (2015) 203-218.
[2] P. Gilon, H.Y. Chae, G.A. Rutter, M.A. Ravier, Calcium signaling in pancreatic beta-cells in health and in Type 2 diabetes, Cell Calcium, 56 (2014) 340-361.
[3] P. Marchetti, R. Lupi, S. Del Guerra, M. Bugliani, L. Marselli, U. Boggi, The beta-cell in human type 2 diabetes, Adv Exp Med Biol, 654 (2010) 501-514.
[4] A.E. Butler, J. Janson, W.C. Soeller, P.C. Butler, Increased beta-cell apoptosis prevents adaptive increase in beta-cell mass in mouse model of type 2 diabetes: evidence for role of islet amyloid formation rather than direct action of amyloid, Diabetes, 52 (2003) 2304-2314.
[5] J. Rahier, Y. Guiot, R.M. Goebbels, C. Sempoux, J.C. Henquin, Pancreatic beta-cell mass in European subjects with type 2 diabetes, Diabetes Obes Metab, 10 Suppl 4 (2008) 32-42.
[6] G.A. Rutter, Visualising insulin secretion. The Minkowski Lecture 2004, Diabetologia, 47 (2004) 1861-1872.
[7] S.E. Kahn, S. Zraika, K.M. Utzschneider, R.L. Hull, The beta cell lesion in type 2 diabetes: there has to be a primary functional abnormality, Diabetologia, 52 (2009) 1003-1012.
[8] T. Scully, Diabetes in numbers, Nature, 485 (2012) S2-3.
[9] P. Detimary, G. Van den Berghe, J.C. Henquin, Concentration dependence and time course of the effects of glucose on adenine and guanine nucleotides in mouse pancreatic islets, J Biol Chem, 271 (1996) 20559-20565.
[10] A.I. Tarasov, F. Semplici, M.A. Ravier, E.A. Bellomo, T.J. Pullen, P. Gilon, I. Sekler, R. Rizzuto, G.A. Rutter, The mitochondrial Ca2+ uniporter MCU is essential for glucose-induced ATP increases in pancreatic beta-cells, PLoS One, 7 (2012) e39722.
[11] F.M. Ashcroft, K(ATP) channels and insulin secretion: a key role in health and disease, Biochem Soc Trans, 34 (2006) 243-246.
[12] A.L. Gloyn, E.R. Pearson, J.F. Antcliff, P. Proks, G.J. Bruining, A.S. Slingerland, N. Howard, S. Srinivasan, J.M. Silva, J. Molnes, E.L. Edghill, T.M. Frayling, I.K. Temple, D. Mackay, J.P. Shield, Z. Sumnik, A. van Rhijn, J.K. Wales, P. Clark, S. Gorman, J. Aisenberg, S. Ellard, P.R. Njolstad, F.M. Ashcroft, A.T. Hattersley, Activating mutations in the gene encoding the ATP-sensitive potassium-channel subunit Kir6.2 and permanent neonatal diabetes, N Engl J Med, 350 (2004) 1838-1849.
[13] A.P. Babenko, M. Polak, H. Cave, K. Busiah, P. Czernichow, R. Scharfmann, J. Bryan, L. Aguilar-Bryan, M. Vaxillaire, P. Froguel, Activating mutations in the ABCC8 gene in neonatal diabetes mellitus, N Engl J Med, 355 (2006) 456-466.
[14] A. Szollosi, M. Nenquin, L. Aguilar-Bryan, J. Bryan, J.C. Henquin, Glucose stimulates Ca2+ influx and insulin secretion in 2-week-old beta-cells lacking ATP-sensitive K+ channels, J Biol Chem, 282 (2007) 1747-1756.
[15] M.A. Ravier, M. Nenquin, T. Miki, S. Seino, J.C. Henquin, Glucose controls cytosolic Ca2+ and insulin secretion in mouse islets lacking adenosine triphosphate-sensitive K+ channels owing to a knockout of the pore-forming subunit Kir6.2, Endocrinology, 150 (2009) 33-45.
[16] A. Arredouani, J.C. Henquin, P. Gilon, Contribution of the endoplasmic reticulum to the glucose-induced [Ca(2+)](c) response in mouse pancreatic islets, Am J Physiol Endocrinol Metab, 282 (2002) E982-991.
[17] A. Arredouani, M. Ruas, S.C. Collins, R. Parkesh, F. Clough, T. Pillinger, G. Coltart, K. Rietdorf, A. Royle, P. Johnson, M. Braun, Q. Zhang, W. Sones, K. Shimomura, A.J. Morgan, A.M. Lewis, K.T. Chuang, R. Tunn, J. Gadea, L. Teboul, P.M. Heister, P.W. Tynan, E.A. Bellomo, G.A. Rutter, P. Rorsman, G.C. Churchill, J. Parrington, A. Galione, Nicotinic Acid Adenine Dinucleotide Phosphate (NAADP) and Endolysosomal Two-pore Channels Modulate Membrane Excitability and Stimulus-Secretion Coupling in Mouse Pancreatic beta Cells, J Biol Chem, 290 (2015) 21376-21392.
[18] X. Wang, X. Zhang, X.P. Dong, M. Samie, X. Li, X. Cheng, A. Goschka, D. Shen, Y. Zhou, J. Harlow, M.X. Zhu, D.E. Clapham, D. Ren, H. Xu, TPC proteins are phosphoinositide- activated sodium-selective ion channels in endosomes and lysosomes, Cell, 151 (2012) 372-383.

[19] R. Aarhus, R.M. Graeff, D.M. Dickey, T.F. Walseth, H.C. Lee, ADP-ribosyl cyclase and CD38 catalyze the synthesis of a calcium-mobilizing metabolite from NADP, J Biol Chem, 270 (1995) 30327-30333.
[20] R. Masgrau, G.C. Churchill, A.J. Morgan, S.J. Ashcroft, A. Galione, NAADP: a new second messenger for glucose-induced Ca2+ responses in clonal pancreatic beta cells, Curr Biol, 13 (2003) 247-251.
[21] B.J. Kim, K.H. Park, C.Y. Yim, S. Takasawa, H. Okamoto, M.J. Im, U.H. Kim, Generation of nicotinic acid adenine dinucleotide phosphate and cyclic ADP-ribose by glucagon-like peptide-1 evokes Ca2+ signal that is essential for insulin secretion in mouse pancreatic islets, Diabetes, 57 (2008) 868-878.
[22] D.J. Drucker, B. Yusta, Physiology and pharmacology of the enteroendocrine hormone glucagon-like peptide-2, Annu Rev Physiol, 76 (2014) 561-583.
[23] D.J. Drucker, M.A. Nauck, The incretin system: glucagon-like peptide-1 receptor agonists and dipeptidyl peptidase-4 inhibitors in type 2 diabetes, Lancet, 368 (2006) 1696-1705.
[24] M. Nauck, U. Smith, Incretin-based therapy: how do incretin mimetics and DPP-4 inhibitors fit into treatment algorithms for type 2 diabetic patients?, Best Pract Res Clin Endocrinol Metab, 23 (2009) 513-523.
[25] T. Tsuboi, G. da Silva Xavier, G.G. Holz, L.S. Jouaville, A.P. Thomas, G.A. Rutter, Glucagon-like peptide-1 mobilizes intracellular Ca2+ and stimulates mitochondrial ATP synthesis in pancreatic MIN6 beta-cells, Biochem J, 369 (2003) 287-299.
[26] D.J. Hodson, R.K. Mitchell, E.A. Bellomo, G. Sun, L. Vinet, P. Meda, D. Li, W.H. Li, M. Bugliani, P. Marchetti, D. Bosco, L. Piemonti, P. Johnson, S.J. Hughes, G.A. Rutter, Lipotoxicity disrupts incretin-regulated human beta cell connectivity, J Clin Invest, 123 (2013) 4182-4194.
[27] D.J. Hodson, A.I. Tarasov, S. Gimeno Brias, R.K. Mitchell, N.R. Johnston, S. Haghollahi, M.C. Cane, M. Bugliani, P. Marchetti, D. Bosco, P.R. Johnson, S.J. Hughes, G.A. Rutter, Incretin-modulated beta cell energetics in intact islets of Langerhans, Mol Endocrinol, 28 (2014) 860-871.
[28] P.J. Calcraft, M. Ruas, Z. Pan, X. Cheng, A. Arredouani, X. Hao, J. Tang, K. Rietdorf, L. Teboul, K.T. Chuang, P. Lin, R. Xiao, C. Wang, Y. Zhu, Y. Lin, C.N. Wyatt, J. Parrington, J. Ma, A.M. Evans, A. Galione, M.X. Zhu, NAADP mobilizes calcium from acidic organelles through two-pore channels, Nature, 459 (2009) 596-600.
[29] E. Brailoiu, T. Rahman, D. Churamani, D.L. Prole, G.C. Brailoiu, R. Hooper, C.W. Taylor, S. Patel, An NAADP-gated two-pore channel targeted to the plasma membrane uncouples triggering from amplifying Ca2+ signals, J Biol Chem, 285 (2010) 38511-38516.
[30] S.W. Tsaih, K. Holl, S. Jia, M. Kaldunski, M. Tschannen, H. He, J.W. Andrae, S.H. Li, A. Stoddard, A. Wiederhold, J. Parrington, M. Ruas da Silva, A. Galione, J. Meigs, R.G. Hoffmann, P. Simpson, H. Jacob, M. Hessner, L.C. Solberg Woods, Identification of a novel gene for diabetic traits in rats, mice, and humans, Genetics, 198 (2014) 17-29.
[31] M. Ruas, L.C. Davis, C.C. Chen, A.J. Morgan, K.T. Chuang, T.F. Walseth, C. Grimm, C. Garnham, T. Powell, N. Platt, F.M. Platt, M. Biel, C. Wahl-Schott, J. Parrington, A. Galione, Expression of Ca(2)(+)-permeable two-pore channels rescues NAADP signalling in TPC-deficient cells, EMBO J, 34 (2015) 1743-1758.
[32] B. Thorens, D. Tarussio, M.A. Maestro, M. Rovira, E. Heikkila, J. Ferrer, Ins1(Cre) knock-in mice for beta cell-specific gene recombination, Diabetologia, 58 (2015) 558-565.
[33] M. Kone, T.J. Pullen, G. Sun, M. Ibberson, A. Martinez-Sanchez, S. Sayers, M.S. Nguyen-Tu, C. Kantor, A. Swisa, Y. Dor, T. Gorman, J. Ferrer, B. Thorens, F. Reimann, F. Gribble, J.A. McGinty, L. Chen, P.M. French, F. Birzele, T. Hildebrandt, I. Uphues, G.A. Rutter, LKB1 and AMPK differentially regulate pancreatic beta-cell identity, FASEB J, 28 (2014) 4972-4985.
[34] B. Brouwers, G. de Faudeur, A.B. Osipovich, L. Goyvaerts, K. Lemaire, L. Boesmans, E.J. Cauwelier, M. Granvik, V.P. Pruniau, L. Van Lommel, J. Van Schoors, J.S. Stancill, I. Smolders, V. Goffin, N. Binart, P. in't Veld, J. Declercq, M.A. Magnuson, J.W. Creemers, F. Schuit, A. Schraenen, Impaired islet function in commonly used transgenic mouse lines due to human growth hormone minigene expression, Cell Metab, 20 (2014) 979-990.
[35] G. Sun, R. Reynolds, I. Leclerc, G.A. Rutter, RIP2-mediated LKB1 deletion causes axon degeneration in the spinal cord and hind-limb paralysis, Dis Model Mech, 4 (2011) 193-202.

[36] D. Oropeza, N. Jouvet, L. Budry, J.E. Campbell, K. Bouyakdan, J. Lacombe, G. Perron, V. Bergeron, J.C. Neuman, H.K. Brar, R.J. Fenske, C. Meunier, S. Sczelecki, M.E. Kimple, D.J. Drucker, R.A. Screaton, V. Poitout, M. Ferron, T. Alquier, J.L. Estall, Phenotypic characterization of MIP-CreERT1Lphi mice with transgene-driven islet expression of human growth hormone, Diabetes, (2015).
[37] B. Wicksteed, M. Brissova, W. Yan, D.M. Opland, J.L. Plank, R.B. Reinert, L.M. Dickson, N.A. Tamarina, L.H. Philipson, A. Shostak, E. Bernal-Mizrachi, L. Elghazi, M.W. Roe, P.A. Labosky, M.G. Myers, Jr., M. Gannon, A.C. Powers, P.J. Dempsey, Conditional gene targeting in mouse pancreatic ss-Cells: analysis of ectopic Cre transgene expression in the brain, Diabetes, 59 (2010) 3090-3098.
[38] A. Solomou, G. Meur, E. Bellomo, D.J. Hodson, A. Tomas, S. Migrenne Li, E. Philippe, P.L. Herrera, C. Magnan, G.A. Rutter, The Zinc Transporter Slc30a8/ZnT8 Is Required in a Subpopulation of Pancreatic alpha-Cells for Hypoglycemia-induced Glucagon Secretion, J Biol Chem., 290 (2015) 21432-21442. doi: 21410.21074/jbc.M21115.645291. Epub 642015 Jul 645215.
[39] A.A. Elayat, M.M. el-Naggar, M. Tahir, An immunocytochemical and morphometric study of the rat pancreatic islets, J Anat, 186 (Pt 3) (1995) 629-637.
[40] C. Benner, T. van der Meulen, E. Caceres, K. Tigyi, C.J. Donaldson, M.O. Huising, The transcriptional landscape of mouse beta cells compared to human beta cells reveals notable species differences in long non-coding RNA and protein-coding gene expression, BMC Genomics, 15 (2014) 620.
[41] M. Yamasaki, R. Masgrau, A.J. Morgan, G.C. Churchill, S. Patel, S.J. Ashcroft, A. Galione, Organelle selection determines agonist-specific Ca2+ signals in pancreatic acinar and beta cells, J Biol Chem., 279 (2004) 7234-7240. Epub 2003 Dec 7232.
[42] E. Brailoiu, J.L. Hoard, C.M. Filipeanu, G.C. Brailoiu, S.L. Dun, S. Patel, N.J. Dun, Nicotinic acid adenine dinucleotide phosphate potentiates neurite outgrowth, J Biol Chem., 280 (2005) 5646-5650. Epub 2004 Nov 5644.
[43] N.P. Kinnear, F.X. Boittin, J.M. Thomas, A. Galione, A.M. Evans, Lysosome-sarcoplasmic reticulum junctions. A trigger zone for calcium signaling by nicotinic acid adenine dinucleotide phosphate and endothelin-1, J Biol Chem., 279 (2004) 54319-54326. Epub 52004 Aug 54325.
[44] S.J. Pitt, T.M. Funnell, M. Sitsapesan, E. Venturi, K. Rietdorf, M. Ruas, A. Ganesan, R. Gosain, G.C. Churchill, M.X. Zhu, J. Parrington, A. Galione, R. Sitsapesan, TPC2 is a novel NAADP-sensitive Ca2+ release channel, operating as a dual sensor of luminal pH and Ca2+, J Biol Chem., 285 (2010) 35039-35046. doi: 35010.31074/jbc.M35110.156927. Epub 152010 Aug 156918.
[45] E. Brailoiu, D. Churamani, X. Cai, M.G. Schrlau, G.C. Brailoiu, X. Gao, R. Hooper, M.J. Boulware, N.J. Dun, J.S. Marchant, S. Patel, Essential requirement for two-pore channel 1 in NAADP-mediated calcium signaling, J Cell Biol., 186 (2009) 201-209. doi: 210.1083/jcb.200904073. Epub 200902009 Jul 200904020.
[46] O.A. Ogunbayo, Y. Zhu, D. Rossi, V. Sorrentino, J. Ma, M.X. Zhu, A.M. Evans, Cyclic adenosine diphosphate ribose activates ryanodine receptors, whereas NAADP activates two-pore domain channels, J Biol Chem., 286 (2011) 9136-9140. doi: 9110.1074/jbc.M9110.202002. Epub 202011 Jan 202007.
[47] X. Zong, M. Schieder, H. Cuny, S. Fenske, C. Gruner, K. Rotzer, O. Griesbeck, H. Harz, M. Biel, C. Wahl-Schott, The two-pore channel TPCN2 mediates NAADP-dependent Ca(2+)-release from lysosomal stores, Pflugers Arch., 458 (2009) 891-899. doi: 810.1007/s00424-00009-00690-y. Epub 02009 Jun 00426.
[48] M. Steen, T. Kirchberger, A.H. Guse, NAADP mobilizes calcium from the endoplasmic reticular Ca(2+) store in T-lymphocytes, J Biol Chem., 282 (2007) 18864-18871. Epub 12007 Apr 18819.
[49] K. Eguchi, I. Manabe, Macrophages and islet inflammation in type 2 diabetes, Diabetes Obes Metab., 15 (2013) 152-158. doi: 110.1111/dom.12168.
[50] G.A. Rutter, D.J. Hodson, Beta cell connectivity in pancreatic islets: a type 2 diabetes target?, Cell Mol Life Sci., 72 (2015) 453-467. doi: 410.1007/s00018-00014-01755-00014. Epub 02014 Oct 00017.

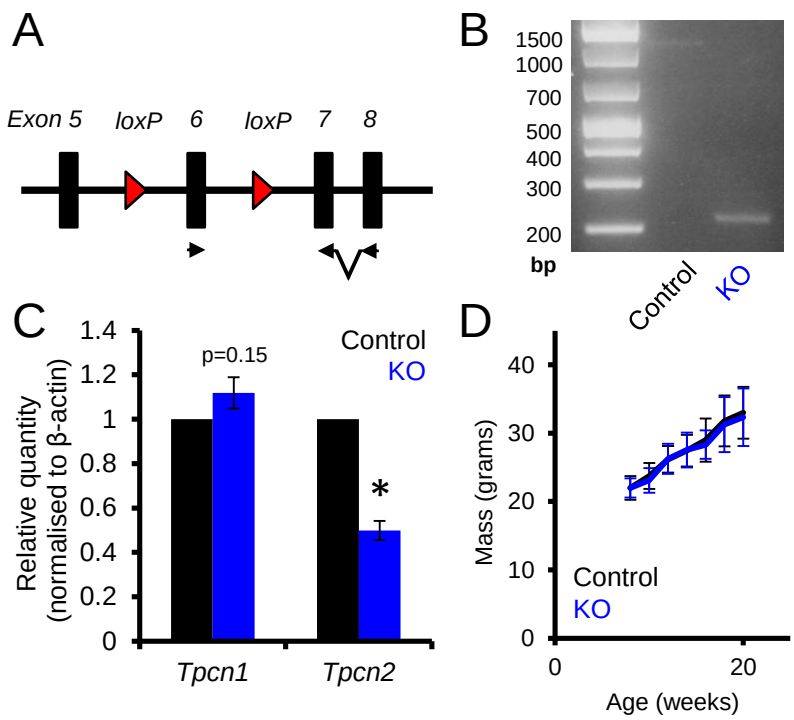

A
Exon 5
loxP
6
loxP
7
8
B
1500
1000
700
500
400
300
200
bp
Control
KO
C
Relative quantity
(normalised to β-actin)
1.4
1.2
1
0.8
0.6
0.4
0.2
0
p=0.15
Control
KO
*
Tpcn1
Tpcn2
D
Mass (grams)
40
30
20
10
0
Control
KO
0
20
Age (weeks)

Figure 1

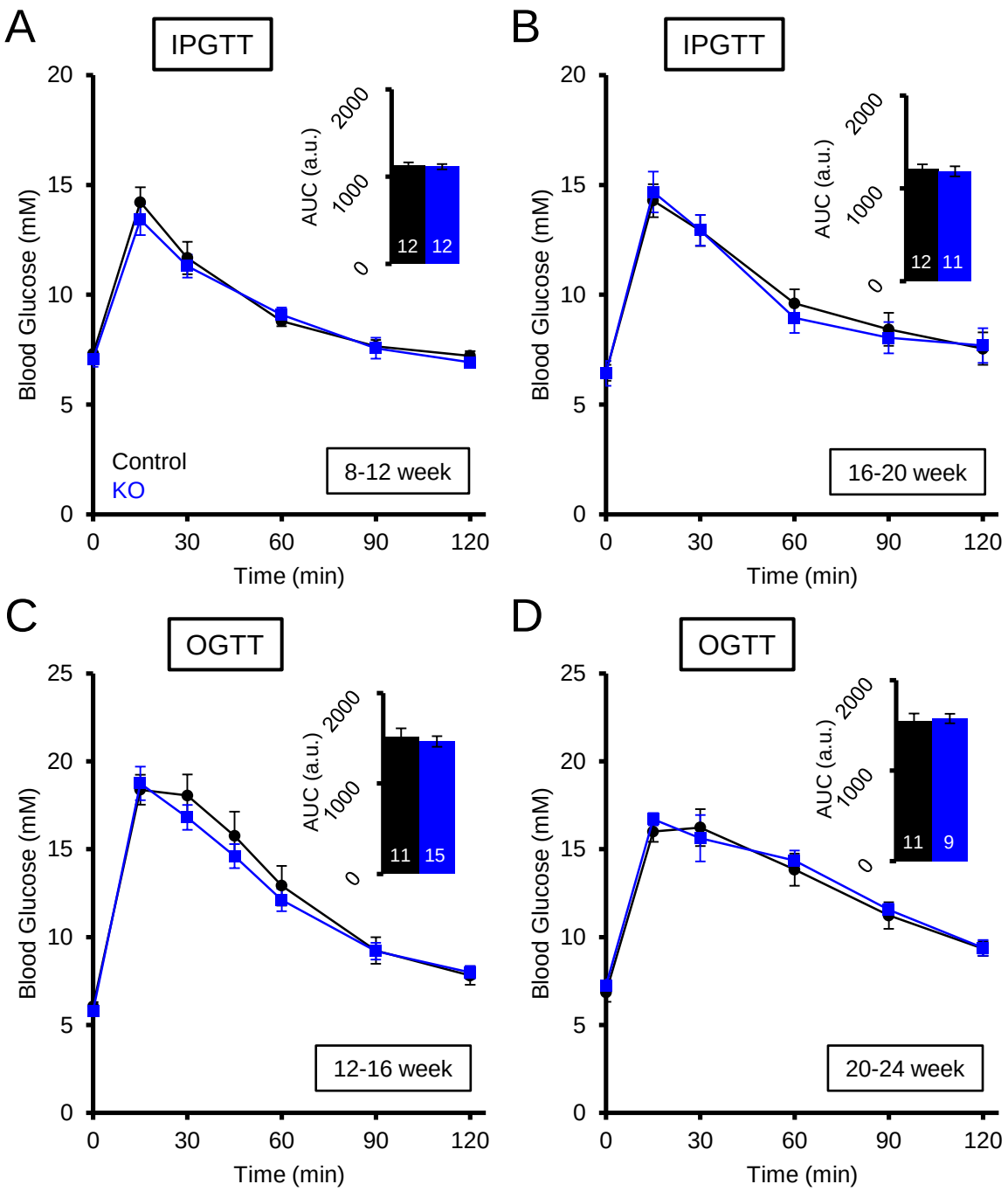

A
IPGTT
Blood Glucose (mM)
Time (min)
AUC (a.u.)
12
12
Control
KO
8-12 week
B
IPGTT
12
11
16-20 week
C
OGTT
11
15
12-16 week
D
OGTT
11
9
20-24 week

Figure 2

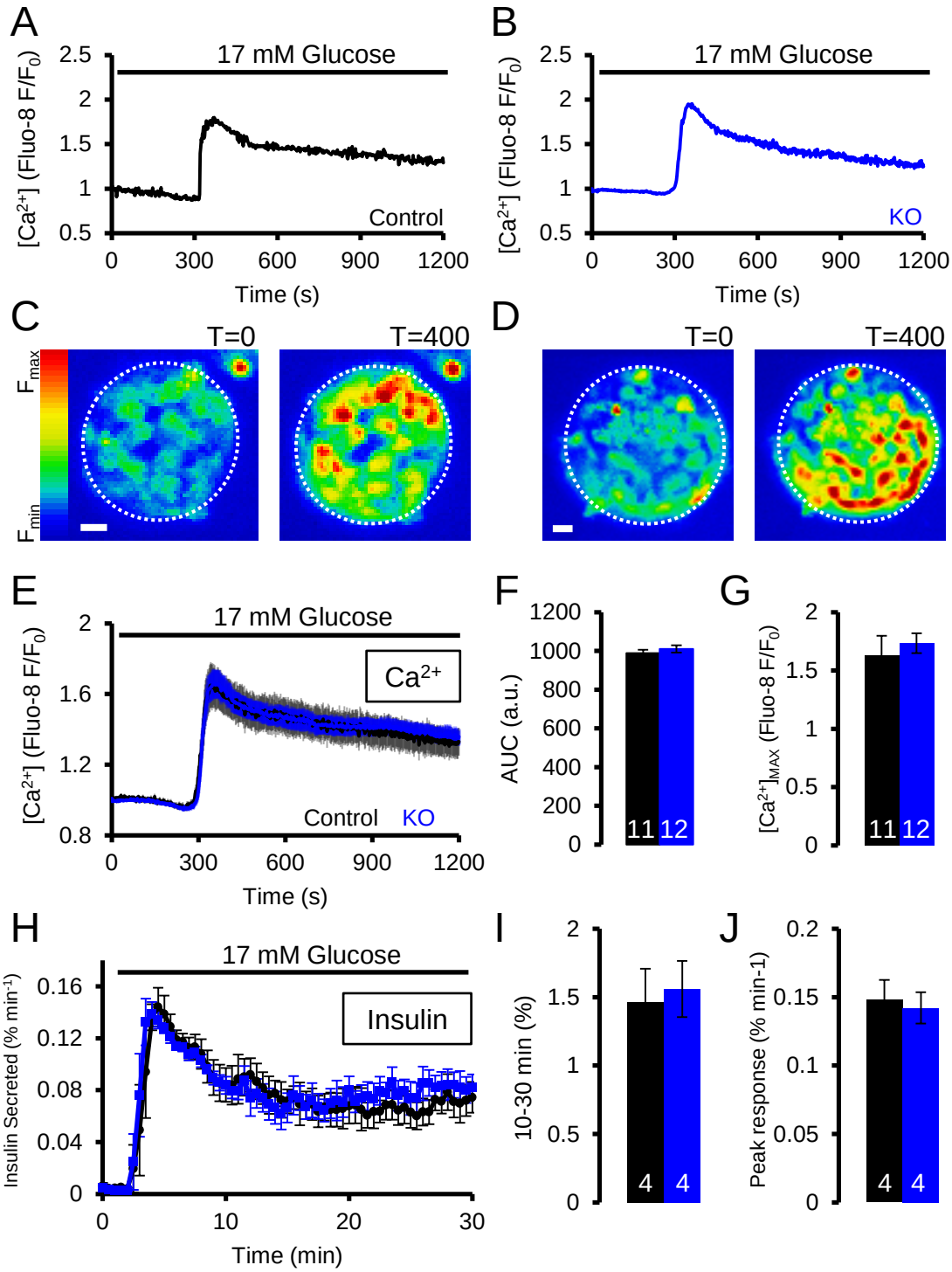

A
17 mM Glucose
Control
[Ca2+] (Fluo-8 F/F0)
Time (s)
B
17 mM Glucose
KO
C
T=0
T=400
Fmax
Fmin
D
E
17 mM Glucose
Ca2+
Control KO
F
AUC (a.u.)
11 12
G
[Ca2+]MAX (Fluo-8 F/F0)
H
Insulin Secreted (% min-1)
Insulin
Time (min)
I
10-30 min (%)
4 4
J
Peak response (% min-1)

Figure 3

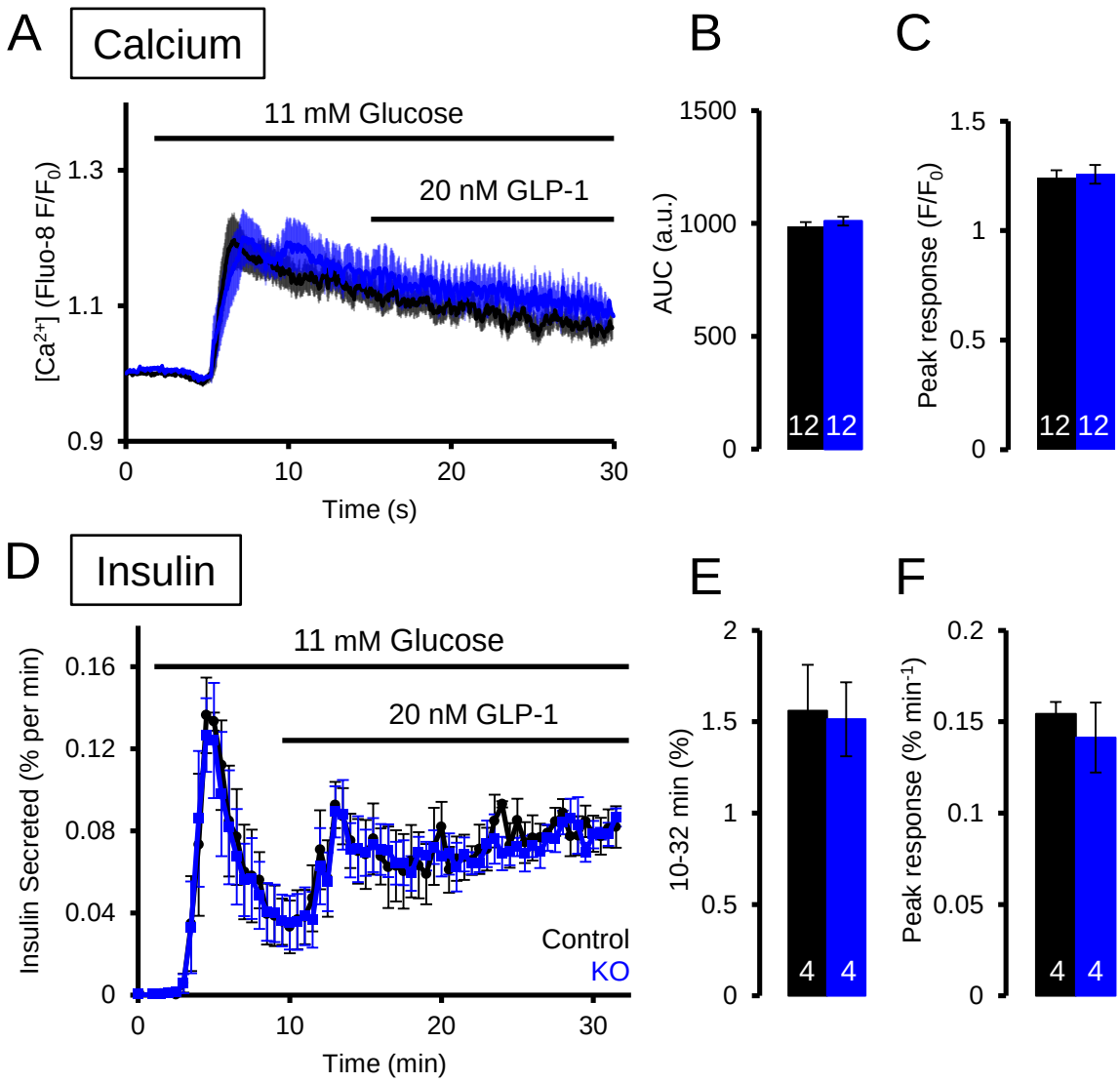

A
Calcium
11 mM Glucose
20 nM GLP-1
[Ca2+] (Fluo-8 F/F0)
1.3
1.1
0.9
0
10
20
30
Time (s)
B
AUC (a.u.)
1500
1000
500
0
12
12
C
Peak response (F/F0)
1.5
1
0.5
0
12
12
D
Insulin
11 mM Glucose
20 nM GLP-1
Insulin Secreted (% per min)
0.16
0.12
0.08
0.04
0
Control
KO
0
10
20
30
Time (min)
E
10-32 min (%)
2
1.5
1
0.5
0
4
4
F
Peak response (% min-1)
0.2
0.15
0.1
0.05
0
4
4

Figure 4

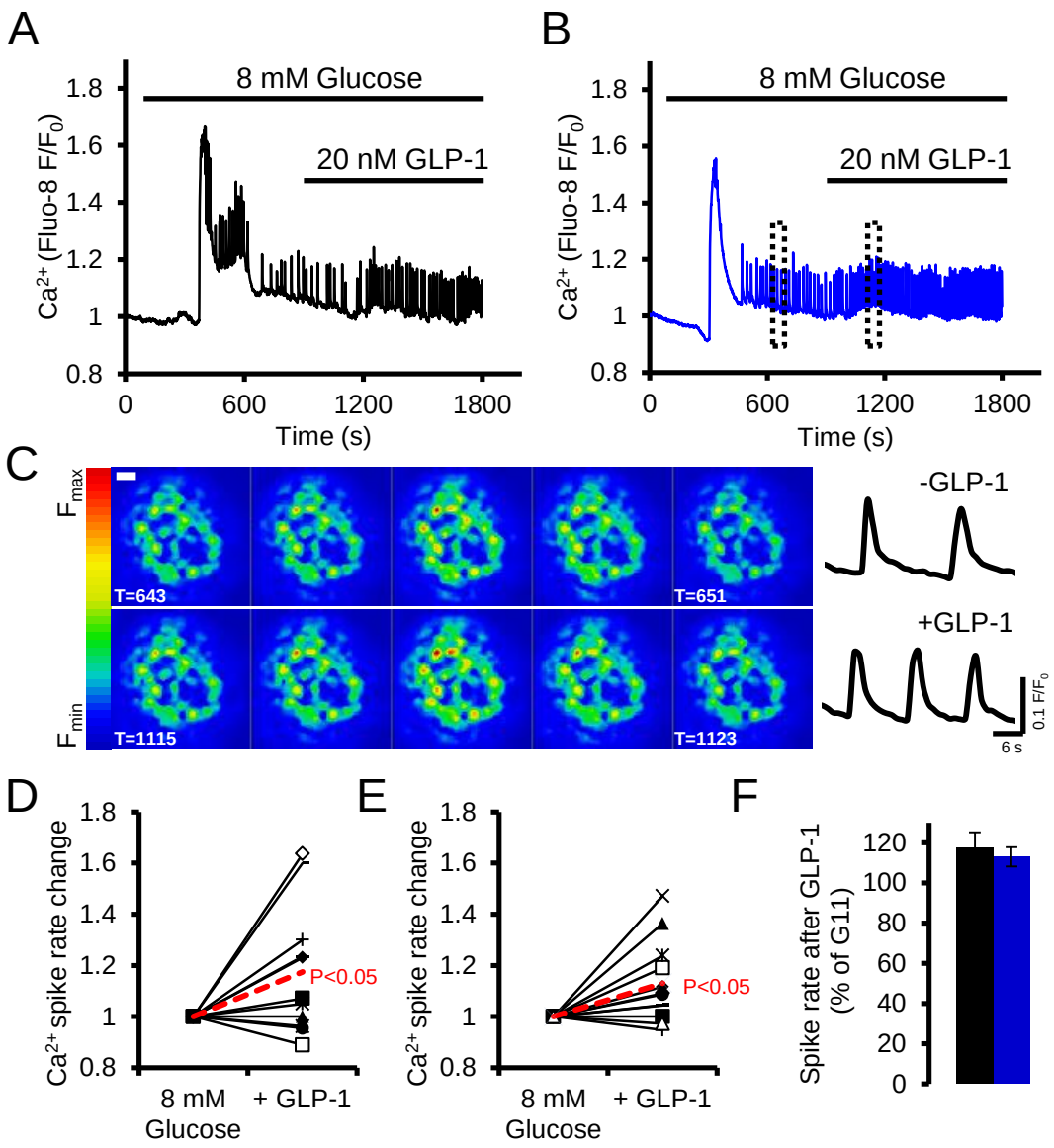

A
8 mM Glucose
20 nM GLP-1
Ca2+ (Fluo-8 F/F0)
Time (s)
B
8 mM Glucose
20 nM GLP-1
Ca2+ (Fluo-8 F/F0)
Time (s)
C
Fmax
Fmin
T=643
T=651
T=1115
T=1123
-GLP-1
+GLP-1
0.1 F/F0
6 s
D
Ca2+ spike rate change
P<0.05
8 mM Glucose
+ GLP-1
E
Ca2+ spike rate change
P<0.05
8 mM Glucose
+ GLP-1
F
Spike rate after GLP-1 (% of G11)

Figure 5